Optical Amplification Characteristics of Cr:LiSAF and Cr:LiCAF under Flashlamp-Pumping

P. Beaud, M. C. Richardson, Y.-F. Chen, and B. H. T. Chai

Abstract— **Small-signal gain measurements of flashlamp-pumped Cr-doped LiSAF and LiCAF are summarized for a range of material parameters. Flashlamp pumping allows efficient energy storage for both materials in the order 1.6 to 2.6% of the electrical pump energy. Small-signal gain values of up to $0.16\,cm^{-1}$ are measured for Cr:LiSAF and $0.09\,cm^{-1}$ for Cr:LiCAF. The gain of both materials is found to be affected by excited state absorption and upconversion. In addition the implications of these results for the design of laser/amplifier systems are discussed.**

I. Introduction

$LiSrAlF_6:Cr^{3+}$ (Cr:LiSAF) [1] and $LiCaAlF_6:Cr^{3+}$ (Cr:LiCAF) [2] are two new additions to a series of new tunable near-infrared laser materials. Currently, the most prominent of these are Ti:sapphire [3] and Alexandrite [4]. Both of these laser materials have attractive laser properties, but they also possess some drawbacks that can be overcome by using Cr:LiSAF or Cr:LiCAF. Ti:sapphire has a high emission cross section and an extremely large emission bandwidth, providing tunable laser radiation from ~700 nm to beyond 1 μm. However, it has a relatively short excited state lifetime of ~3 μs [3], making flashlamp pumping inefficient. A Ti:sapphire laser therefore requires a second laser such as an argon ion laser or a frequency-doubled neodymium laser as a pump source. In contrast to Ti:sapphire, alexandrite can be efficiently pumped with flashlamps, allowing the construction of compact laser and amplifier systems, but this material must be heated above ambient temperature for optimum performance. In addition it suffers from strong thermal lens effects which makes difficult the achievement of high output powers in a diffraction-limited spatial mode [4].

Cr:LiSAF and Cr:LiCAF both possess suitable properties for the generation of high-energy tunable radiation in the near infrared. They exhibit small thermal lensing [5]–[7], a high damage threshold [6] and a sufficiently long upper-state lifetime to ensure efficient energy storage. Furthermore laser rods of diameters up to 25 mm can now be fabricated, an important consideration for the design of high-energy lasers and amplifiers. The relatively long upper-state lifetime of Cr:LiSAF and Cr:LiCAF, 67 μs [1] and 170 μs [2], respectively, makes it possible to efficiently pump these materials with flashlamps. Laser action of flashlamp-pumped Cr:LiSAF [8] and the use of flashlamp-pumped Cr:LiSAF amplifiers for chirped pulse amplification of femtosecond pulses [9]–[14] have been recently demonstrated. Cr:LiSAF and Cr:LiCAF have also been shown to be amenable to diode laser pumping using semiconductor lasers operating near 670 nm [15]–[17] and at 752 nm [18]. However, the technology for high-power generation and amplification using laser diode pumped Cr-doped LiSAF or LiCAF has yet to be developed.

With the development of high-power laser systems using Cr:LiSAF and Cr:LiCAF, it becomes increasingly important to assess the optical gain properties of these materials. Whereas the optical spectroscopic data [1], [2], [19], the crystallographic structure [20], [21] the thermo-mechanical and thermo-optical properties [5]–[7] and the optical damage limits [6] have been studied, no detailed investigation of the small-signal gain properties of these materials has been reported yet to our knowledge. The small-signal gain of both of these materials is moderate compared to Ti:sapphire. Moreover, preliminary results have shown that it is affected by excited-state absorption [22]–[24] and upconversion [23], [25]. For these reasons an exact knowledge of the amplification characteristics of these materials is indispensable for the design of high-power, flashlamp-pumped, laser systems using Cr:LiSAF or Cr:LiCAF. In this paper we report small-signal gain measurements of Cr:LiSAF and Cr:LiSAF under flashlamp pumping, discuss the influence of excited-state absorption (ESA) and upconversion, and present results of radial gain distribution measurements in a large, 25-mm diameter Cr:LiSAF rod. Finally we will discuss the implications of our experimental results for the design of laser/amplifier systems.

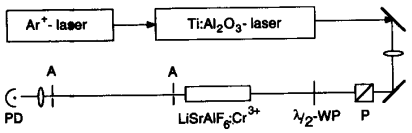

Fig. 1. Experimental set-up. P: polarizer; WP: waveplate; A: aperture; PD: photodiode.

II. Small-Signal Gain Measurements: Experimental Set-Up

The small-signal gain is measured by probing cylindrical rods with a CW Ti:sapphire laser tunable in wavelength from 780 to 900 nm (Fig. 1). This tuning range covers the spectral

Manuscript received March 22, 1993; revised August 2, 1993. This work is supported by the State of Florida and the National Science Foundation under Grant # ECS-9113726.

The authors are with the Center for Research in Electro-Optics and Lasers (CREOL), University of Central Florida, Orlando Florida 32826 USA.

IEEE Log Number 9216380.

emission range of Cr:LiSAF and most of that of Cr:LiCAF. The small-signal gain is measured by probing cylindrical rods of 4 mm diameter and 65 mm length situated in a conventional laser pump cavity. The laser head houses two flashlamps each having an arc length of 56 mm. The axis formed by the flashlamps is orthogonal to the c-axis. The flashlamps are close coupled and surrounded by a high-brilliance magnesium oxide diffuser. The flashlamps are energized by a power supply consisting of a simmer capacitor bank with a capacitance of 30 μF and a controller. The simmer mode operation increases the flashlamp lifetime and pumping efficiency, reduces magnetic interference radiation, and allows the lamp status to be controlled. This unit can operate at a maximum voltage of 1.83 kV and delivers an energy of up to 50 J. The flashlamp pump duration (FWHM) is 130 μs, sufficiently short to efficiently pump the Cr:LiSAF and Cr:LiCAF rods and long enough to ensure the flashlamp lifetime. Although we use as a coolant an equal mixture of water and ethylene glycol to prevent erosion of the crystal [8], we have observed material erosion operating a Cr:LiSAF laser over a long time. After a 12-month period, the diameter of a 1.4% Cr-doped rod has decreased from initially 4 mm to 3.1–3.5 mm, with the greatest material loss occurring at the position of the O-rings.

The small-signal gain is determined by transmitting a small fraction of the Ti:sapphire beam through the rod and measuring the amplification during flashlamp operation using a photodiode and an oscilloscope. Two pinholes separated by approximately 2 m are used to reduce the contribution of fluorescence to the signal. In addition, the remaining fluorescence signal is measured in the absence of the probe beam and is then subtracted from the signal. The two pinholes are adjusted so that they are not clipping the transmitted probe beam, which would be very sensitive to changes to the transmitted beam by pump-induced effects such as thermal lensing or optical bending. Thermal lensing effects in Cr:LiSAF and CR:LiCAF are small [5]–[7]. Moreover, if there would be significant thermal lensing in the rod that could cause enough defocusing to cut part of the probe beam at the exit pinholes, this would lead to transmission changes of the CW probe beam. Such transmission changes of the CW probe beam should be observed in our experiment between the pump intervals since the thermal relaxation time is estimated to be in the order of hundreds of milliseconds, which is much longer than the pump pulse. We do not observe any pump-induced change of the amplitude of the transmitted beam in our experiment. A half-wave plate is used to rotate the polarization of the probe beam, allowing the measurement of the small-signal gain for both polarizations separately. Because the laser pump cavity used in this experiment is optimized to efficiently pump Nd-doped materials, its flowtube is doped with Samarium, which has a strong absorption band at 400 nm that significantly overlaps with the $^4A_2 \rightarrow ^4T_1a$ absorption band of Cr:LiSAF and Cr:LiCAF. We estimate that an approximately 30% higher pump efficiency, as reported in this paper, can be obtained using a laser head optimized to efficiently pump these materials. We have designed double flashlamp-pumped laser modules specifically for Cr:LiSAF and Cr:LiCAF with Cerium-doped glass flashlamps giving better pump efficiencies.

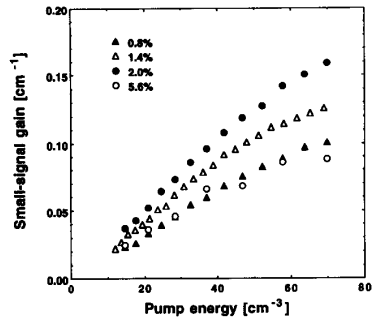

Fig. 2. Small-signal gain at 850 nm versus electrical energy in Cr:LiSAF for π-polarized light for Cr $^{3+}$ concentrations of 0.8, 1.4, 2, and 5.6%.

III. Small-Signal Gain Measurements: Results

A. Small-Signal Gain of Cr:LiSAF

We first measured the small-signal gain of Cr:LiSAF for 0.8%, 2% and 5.6% Cr^{3+}-concentrations. (Note, that all the concentration values used throughout this paper refer to the estimated actual chromium concentration of CrF_3 replacing AlF_3 in the laser rod, and not to that of the initial melt as some authors do.) The results obtained with all four rods are shown in Fig. 2. The incoming light is polarized parallel to the c-axis (π polarization), the polarization with the higher emission cross section. The wavelength is tuned to 850 nm, the maximum of the gain curve. For the 2% sample we measure a small-signal gain value of 0.16 cm^{-1} at a pump energy of 50 J. We expect the optimum dopant concentration for a 4-mm rod to be between 1.4 and 2%. The chromium concentration of the 5.6% sample is clearly too high as shown in Fig. 2. The gain in the center of the rod has decreased compared to the lower-doped samples. The measured single pass loss at 850 nm for the four samples was 7.1%, 15.3%, 13.7%, and 17% for the 0.8%, 1.4%, 2%, and 5.6% samples, respectively. These numbers include also the reflection losses, since the rods were not antireflection-coated. Fig. 2 shows clearly a saturation of the small-signal gain curve with increasing pump energy. As we will discuss in the next section the saturation of the gain with increasing pump energy is mostly due to upconversion [23], [25] but ground-state bleaching, excited-state absorption (ESA) at the pump wavelength [26], and saturation of the flashlamp pump energy may also contribute to this effect.

The spectral dependence of the small-signal gain is shown in Fig. 3 for both polarizations. The maximum gain for π polarization is found around 850 nm, as is expected from the previously published wavelength dependence of the emission cross section [1]. The steeper decay of the gain towards lower wavelengths is due to the increasing edge of the broad absorption band centered at 640 nm corresponding to the $^4A_2 - {}^4T_2$ transition, the transition from the ground state into the upper laser level. The wavelength dependence of the emission for σ polarization is identical to that for π polarization, but with a three times smaller cross section [1].

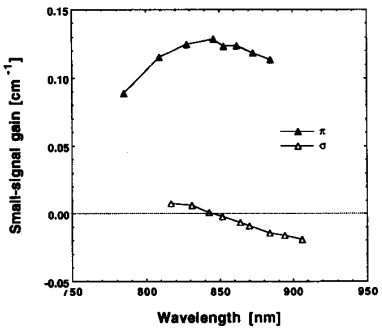

Fig. 3. Small-signal gain of Cr:LiSAF versus wavelength at an electrical input energy of 50 J for both polarizations.

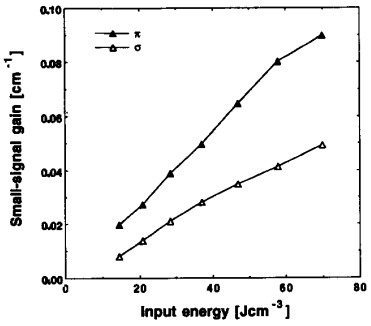

Fig. 4. Small-signal gain of the 2.5% chromium-doped LiCAF rod at 785 nm versus electrical input energy for both polarizations.

We therefore would expect the small-signal gain values for σ polarization to be approximately one third of those of the π polarization. Surprisingly (at first sight), as shown in the lower curve in Fig. 3, the small-signal gain value for σ-polarization is an order of magnitude smaller than for the π polarization and decreases linearly with increasing wavelength. Moreover the gain becomes negative for wavelengths above 845 nm. This serious pump-induced loss mechanism is due to excited-state absorption, as we will discuss in more detail in section IV.A.

An interesting property of a new laser material is its capacity to efficiently store the input energy. Our results demonstrate for π -polarization a maximum small-signal gain of 0.16 cm^{-1} at an electrical input energy of 50 J for a rod having chromium concentration of 2%. Using this value and the effective gain cross section, which we will evaluate in section IV.A, of $3.2 \cdot 10^{-20}$ cm^2 we obtain an inversion density $n = g/\sigma_{\text{eff}}$ of $5 \cdot 10^{18}$ cm^{-3} (g is the measured small-signal gain). This corresponds to an inversion of 2.8% of the Cr ions and to a stored energy density of 1.2 Jcm^{-3} in the center of the rod. Assuming a homogeneous pumping (we estimate that homogeneous pumping is achieved for Cr concentrations between 1.4 and 2% for 4-mm rod diameter) we calculate with these numbers an overall pump efficiency (stored energy versus electrical input) of 1.6%. The corresponding values for the stored energy in the center of the rod at the same pumping level are 0.92 Jcm^{-3} and 0.73 Jcm^{-3} for the 0.8% and 1.4% doped rods, respectively.

B. Small-Signal Gain of Cr:LiCAF

Fig. 4 shows the small-signal gain of Cr:LiCAF versus electrical input energy for both polarizations. The actual chromium concentration in the rod is 2.6% and the probe wavelength is tuned to 785 nm close to the maximum of the gain curve at 780 nm. A small-signal gain value of 0.09 cm^{-1} for π polarization and 0.05 cm^{-1} for σ polarization was measured at a pump energy of 50 J. The saturation of the gain with increasing pump energy is much less pronounced than that observed with Cr:LiSAF (see Fig. 2). In contrast to Cr:LiSAF the passive losses in Cr:LiCAF were found to be significantly dependent on the polarization. The measured single-pass losses, including the reflection losses, are 25% and 15% for the π and σ polarization, respectively. At the present time we do not understand this significant polarization dependence of the loss.

The small-signal gain was 0.09 cm^{-1} at an electrical input energy of 50 J for a chromium concentration of 2.5%. Using this value and the effective gain cross section, which we will evaluate in section IV.C, of 8.9×10^{-21} cm^2 [2] we deduce an inversion density $n = g/\sigma_{\text{eff}}$ of 1×10^{19} cm^{-3}. This corresponds to an inversion of 2.9% of the Chromium ions and to a stored energy density of 2.6 Jcm^{-3}. Assuming homogeneous pumping we calculate with these values an overall pump efficiency (stored energy versus electrical input) of 3.6%. Due to the longer upper state lifetime the stored energy in Cr:LiCAF of 2.6 Jcm^{-3} at a pump energy of 50 J is significantly higher than the corresponding value of 1.2 Jcm^{-3} of the 2% doped Cr:LiSAF rod. (Because of its significantly lower absorption cross section, a 2.6% Cr:LiCAF rod has approximately the same pump light absorption as a ~1.8% Cr:LiSAF rod.) While its storage efficiency is higher, the measured small signal gain of Cr:LiCAF of 0.09 cm^{-1} is significantly lower than the corresponding value of 0.16 for the 2% Cr:LiSAF rod.

The wavelength dependence of the small-signal gain of Cr:LiCAF is shown in Fig. 5 for both polarizations. The maximum gain of this material occurs at a wavelength of ~780 nm [2]. Unfortunately, the small-signal gain Ti:sapphire probe laser did not cover the complete spectral range of Cr:LiCAF. However, we are able to measure the small-signal gain of Cr:LiCAF over a large range from 780 to 920 nm. In this spectral range the gain decreases with increasing wavelength. At approximately 895 nm for π-polarized light and at 865 nm for σ-polarized light the small-signal gain becomes negative. As explained in Section III.B, we believe this to be a strong indication of excited-state absorption.

C. Gain Distribution in a 25-mm-Diameter Cr:LiSAF Rod

In order to use Cr:LiSAF as an amplifier, a knowledge of the gain distribution throughout the whole aperture of the rod is of special interest. We measured the gain distribution on a large-aperture Cr:LiSAF rod with a diameter of 25 mm and a length of 118 mm. This rod was fabricated from a single boule of Cr:LiSAF measuring approximately 130 mm long by 35 mm diameter. The rod is of good optical quality. A wave

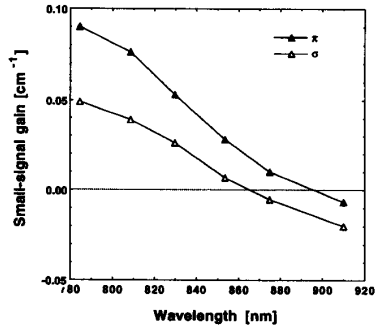

Fig. 5. Small-signal gain of Cr:LiCAF versus wavelength at an electrical input energy of 50 J for both polarizations.

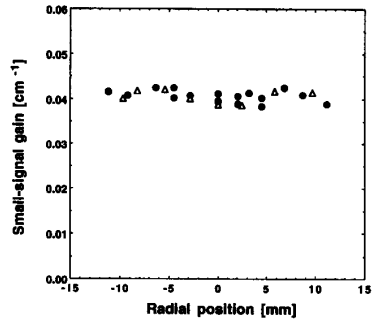

Fig. 6. Measured gain distribution of the 25-mm-dimeter Cr:LiSAF rod at a pump energy of 1.8 kJ. The circles and the triangles represent data by translating the beam along and perpendicular to the c-axis.

distortion of less than a 1/2 wave rms is measured across the aperture over the full length of the rod. Although the rod contained the boule core, no beam deteriorating effects were observed in the center of the rod. The gain distribution was measured with a 200-mm long 8-flashlamp, close-coupled amplifier module operating in a single-shot mode with a maximum electrical input energy of 5 kJ in a 300-μs-long flashlamp pulse. For this pumping configuration we found a homogeneous gain distribution for a chromium concentration of 0.6% (chromium replacing aluminum). The measured gain distribution is homogeneous over the whole aperture of the rod, as shown in Fig. 6.

IV. Excited State Absorption and Upconversion

The polarization of the small-signal gain of Cr:LiSAF observed in the small-signal gain experiments strongly suggest that a significant loss mechanism is present in this laser material. As we will discuss in this section this loss mechanism can be interpreted as a result of ESA. ESA at the laser wavelength significantly reduces the small-signal gain, which in presence of ESA is given by

$$g = N_2(\sigma_e - \sigma_{\mathrm{ESA}}) \tag{4.1}$$

where σ_e is the emission cross section and σ_{ESA} the cross section for excited state absorption. We will show that ESA at the emission wavelengths leads to a reduction of the gain

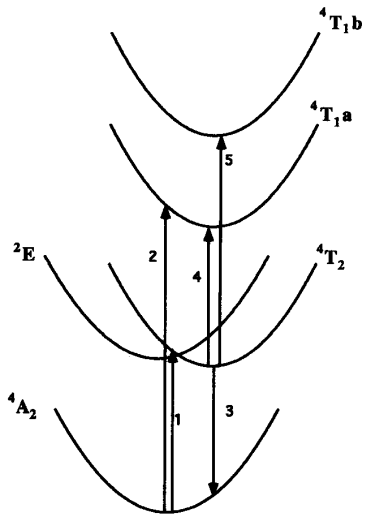

Fig. 7. Schematic energy ban diagram for Cr:LiSAF and Cr:LiCAF. Shown as arrows in the figure are the two main absorption transitions 1, 2), the laser transition 3), and the ESA transitions overlapping with the emission 4) and pump 5) bands.

for π-polarized light of approximately 30% for Cr:LiSAF and 26% for Cr:LiCAF. Other effects, which may affect the optical gain of a material, such as ESA at the pump wavelengths and upconversion, will also be briefly discussed in this section. Fig. 7 shows a schematic energy band diagram of Cr:LiSAF and Cr:LiCAF to facilitate the discussion in this

A. ESA in Cr:LiSAF

The small-signal gain measurements for σ-polarization show that the gain at this polarization is more or less canceled over the whole emission range of Cr:LiSAF. As we have discussed in [24] this loss mechanism is due to excited-state absorption (ESA) from the $^4\mathrm{T}_2$ to the $^4\mathrm{T}_1\mathrm{a}$ excited state. ESA at the emission wavelength reduces the emission cross section to an effective gain cross section σ_{eff}, which is given by

$$\sigma_{\mathrm{eff}}^{\pi,\sigma}(\lambda) = \sigma_e^{\pi,\sigma}(\lambda) - \sigma_{\mathrm{ESA}}^{\pi,\sigma}(\lambda) = \frac{g^{\pi,\sigma}(\lambda)}{N_2} \tag{4.2}$$

where the upper scripts stand for the two polarization states. N_2 is the density of the upper level population, and g is the measured small-signal gain. The σ-polarized gain becomes negative at ~845 nm (see Fig. 3 lower curve). At this wavelength the excited-state absorption cross section σ_{ESA} therefore equals the emission cross section. From the knowledge of the latter at this wavelength [1] the ESA cross section is $\sigma_{\mathrm{ESA}}^{\sigma} = \sigma_e^{\sigma} = 1.6 \cdot 10^{-20}\,\mathrm{cm}^2$.

Although ESA suppresses the gain of Cr:LiSAF for σ-polarized light, there is no evidence of strong ESA for π-polarized light. However ESA may lead to some reduction in the small-signal gain for π-polarization. Theoretical predictions [27] suggest that the ESA cross section $\sigma_{\mathrm{ESA}}(\lambda)$ is unpolarized for Cr:LiCAF. Since Cr:LiSAF is a very similar

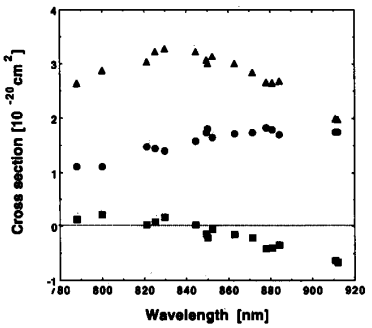

Fig. 8. Wavelength dependence of the ESA cross section (circles) and of the effective gain cross section for π (triangles) and σ polarizations (squares) of Cr:LiSAF.

crystal, we can expect that ESA in Cr:LiSAF is likewise independent of polarization [28]. Under this assumption, and using the value of σ_{ESA} evaluated above, the emission cross section σ_e^{π} of $4.8 \cdot 10^{-20}\,\mathrm{cm}^2$ for π-polarization at 845 nm [1] reduces by ~33% to an effective gain cross section $\sigma_{\mathrm{eff}}^{\pi}\,(= \sigma_e^{\pi} - \sigma_{\mathrm{ESA}})$ of $3.2 \cdot 10^{-20}\,\mathrm{cm}^2$. Approximately 30% larger values for the ESA cross section of Cr:LiSAF have been reported in [23] performing a similar experiment with higher-doped Cr:LiSAF, somewhat higher pump densities, and using a laser pump source instead of flashlamp pumping. It is not clear to us if these differences may explain the discrepancy in the experimental result. Our result, however, is in good agreement with a recent publication [1] where the intrinsic slope efficiency of a Cr:LiSAF laser was found to be ~30% lower than the quantum-defect-efficiency.

With the asumption that the ESA cross section is independent of polarization we can also deduce the wavelength dependence of σ_{ESA} by dividing $\sigma_{\mathrm{eff}}^{\pi}$ with $\sigma_{\mathrm{eff}}^{\sigma}$ and using (4.1), which results in:

$$\sigma_{\mathrm{ESA}}(\lambda) = \frac{\sigma_e^{\pi}(\lambda)\, g^{\sigma}(\lambda) - \sigma_e^{\sigma}(\lambda)\, g^{\pi}(\lambda)}{g^{\sigma}(\lambda) - g^{\pi}(\lambda)} \tag{4.3}$$

By using the measured small-signal gain values $g^{\pi,\sigma}$ and the previously published emission spectra [1] we can determine with (4.3) the wavelength dependence of the ESA cross section. The results are plotted in Fig. 8. The figure likewise includes the effective gain cross sections for both polarizations which can be obtained using (4.2).

The measurements shown in Fig. 2 show a significant saturation of the small-signal gain at higher pump levels for Cr:LiSAF. There are several effects that can result in such a saturation, namely ground-state bleaching, excited-state absorption of the pump light, and upconversion. Including these effects, the rate equation is given by:

$$\frac{dN_2}{dt} = \int_{\lambda}\int_{t} P(t,\lambda)\{\sigma_a(\lambda) - N_2\sigma_{\mathrm{ESA}}(\lambda)\}\, dt\, d\lambda - \frac{N_2}{\tau_2} - \alpha N_2^2 \tag{4.4}$$

where $P(t,\lambda)$ is the optical flashlamp pump pulse, N is the chromium density, σ_a is the absorption cross section, τ_2 is the upper-state lifetime and α is a coefficient describing upconversion. The first term on the right-hand side of (4.4) describes the absorption of the pump light, including depletion of the pump level and excited, state absorption. The second term describes the lifetime of the excited state, and the last term describes the upconversion process, which has a square dependence of excited-state density [25].

Cr:LiSAF has a significant ESA absorption band around 500 nm with a bandwidth of approximately 100 nm and a maximum cross section of $3 \cdot 10^{-20}$ cm^2 [26]. This absorption band can be assigned to the $^4\mathrm{T}_2 \rightarrow ^4\mathrm{T}_1\mathrm{b}$ excited-state transition [27]. Although this cross section is comparable in magnitude with the absorption cross section of the ground state, in our experiment only a few percent of the chromium atoms are inverted, and we can conclude that ESA at the pump wavelengths leads to a negligible contribution to the gain saturation observed in our experiment. For the same reason ground-state bleaching plays likewise a minor role and leads to a gain saturation of only a few percent.

B. Upconversion in Cr:LiSAF

Quantitative measurements of the upconversion process in Cr:LiSAF have recently been reported, resulting in values of α of $11 \cdot 10^{-16}$ cm^3 s^{-1} [25] and between 3.5 and $30 \cdot 10^{-16}$ cm^{3}sec^{-1}, depending on the chromium concentration [24]. To test if the saturation of the gain at higher pump energies, as observed in our gain experiments (see Fig. 2), is due to upconversion and not just due to the saturation of the pulse forming network, we exchange the 30-μF capacitor with a 100-μF capacitor bank allowing us to double the pump energy. The result of a 2% doped rod is shown in Fig. 9. The solid triangles correspond to data taken with the 30-μF capacitor bank and the empty triangles with the 100-μF capacitor bank. The fit (dashed line in Fig. 9) has been calculated using (4.4), assuming a Gaussian shape of the pump pulse and neglecting the pump ESA. The fit result in a value for α of $17 \cdot 10^{-16}$ cm^{3}s^{-1} which is significantly higher than those previously reported [23], [25]. This difference may be due to the fact that a part of the gain saturation may be still due to saturation of the flashlamps, pump ESA, and the fact that in the laser head used in this experiment the pump radiation is filtered by samarium. Samarium has an absorption band in the blue/UV part of the spectrum that partially overlaps with the $^4\mathrm{T}_2 \rightarrow ^4\mathrm{T}_1\mathrm{a}$ absorption band of Cr:LiSAF. Increasing the current density in the flashlamps tends to shift the emission spectrum of the emitted light towards the blue/UV part of the spectrum. Despite those discrepancies we believe that upconversion is the main contributor to the observed linear amplification characteristic observed in Cr:LiSAF amplifiers [10], [11].

C. ESA in Cr:LiCAF

ESA in Cr:LiCAF has already been investigated in detail by Lee *et al.* [27]. These authors reported the absorption of the $^4\mathrm{T} \rightarrow ^4\mathrm{T}_1\mathrm{b}$ excited-state transition. This absorption band

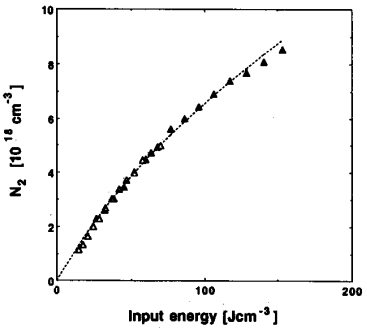

Fig. 9. Inversion density of 2% chromium-doped LiSAF versus electrical input energy. Solid triangles: data taken with 30- μF capacitor bank; empty triangles: data obtained with 100- μF capacitor bank; dashed line: fit using (4.4) (see text).

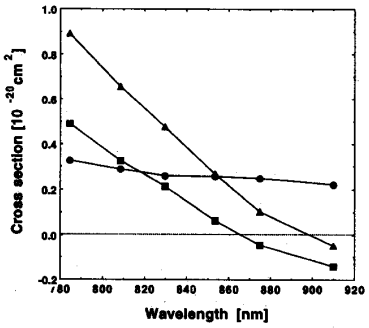

Fig. 10. Wavelength dependence of the ESA cross section (circles) and of the effective gain cross section for π (triangles) and σ polarization (squares) of Cr:LiCAF.

has a maximum at 500 nm with a bandwidth of approximately 100 nm and an absorption cross section of $1.6 \cdot 10^{-20}$ cm^2. In the same paper [27] two Jahn–Teller split components of the $^4T_2 \rightarrow ^4T_1$a excited-state transition are theoretically predicted. The first of these ESA bands, which has nonsymmetric transition matrix elements for π and σ polarization, has not been observed [27]. The second $^4T_2 \rightarrow ^4T_1$a excited-state transition is predicted to be independent of polarization and has been experimentally observed showing an increasing ESA band by decreasing the wavelength from 1.5 to 1 μm [27]. At 1 μm the ESA cross section is $1.6 \cdot 10^{-21}$ cm^2 [27]. However, because the spectral range of their measurements was limited to wavelengths longer than 1 μm, they were not able to resolve the maximum of this transition band. Our measurements indicate that ESA may continuously increase with decreasing wavelength from 1 μm towards 780 nm.

Following the theoretical discussion of [27] we can therefore assume that the ESA cross section is independent of polarization. With (4.3) and the experimentally measured values of the small-signal gain, we can determine the cross section of the ESA and the effective gain cross sections for both polarizations. The results are shown in Fig. 10. The ESA cross section linearly decreases from $3.2 \cdot 10^{-21}$ cm^2 to $2.2 \cdot 10^{-21}$ cm^2 by increasing the wavelength from 785 to 910 nm. By extrapolating these data to a wavelength of 1 μm, we obtain an ESA cross section of $\sim 1.5 \cdot 10^{-21}$ cm^2, which closely corresponds to the previously measured value of $1.6 \cdot 10^{-21}$ cm^2 at this wavelength [27]. Our results suggest that the emission cross section for π polarization at 785 nm of $1.21 \cdot 10^{-20}$ cm^2 [1] reduces to an effective gain cross section of $8.9 \cdot 10^{-21}$ cm^2. This corresponds to a decrease of the small-signal gain of 26%. Taking experimental uncertainties into account, this result agrees quite well with an earlier finding [2] where the intrinsic slope efficiency of a Cr:LiCAF laser was found to be $\sim$20% lower than the quantum-defect efficiency.

For Cr:LiCAF the saturation of the gain at higher pump energies is less obvious than observed in Cr:LiSAF (see Fig. 4). Thus we believe that upconversion has less of an effect on the small-signal gain for this material. This conclusion is supported by the fact that the values for α reported in the literature are approximately a factor of 4 lower than those for Cr:LiSAF [25].

V. Implications for Amplifier Design

A. Polarizations

The strong polarization of the small-signal gain observed for Cr:LiSAF has strong implications for the design of high-power oscillator–amplifier systems. In these systems amplifiers are configured in such a way as to maximize their energy extraction, and minimize ASE and the amplification of retro-reflected laser light. In many amplifier system designs, this involves utilizing the gain properties of both polarizations. Clearly from the measurements described here, this is a limitation for Cr:LiSAF. Although the small-signal gain of Cr:LiCAF is less polarized than that of Cr:LiSAF, it is significantly lower than that of Cr:LiSAF, and it will be difficult to build optical amplifiers using this material.

B. Gain

To illustrate the consequences of ESA and upconversion to the design of Cr:LiSAF amplifiers, we can compare the gain properties of Cr:LiSAF to that of Nd:glass, which is maybe the most prominent solid-state laser material for the construction of multistage amplifier systems. Nd:glass has an emission cross section of $4 \cdot 10^{-20}$ cm^2, close to that of Cr:LiSAF of $5 \cdot 10^{-20}$ cm^2. We would therefore expect the performance of Cr:LiSAF amplifiers to be similar to Nd:glass amplifiers. However, there are several aspects, namely ESA and upconversion, that limit the gain available from Cr:LiSAF amplifiers, which makes it more difficult to build as efficient amplifiers than is the case with Nd:glass.

ESA not only cancels the small-signal gain for σ-polarized light, but also reduces the gain of the π-polarization by $\sim$30%. At first sight this problem could be simply overcome by increasing the pump energy by $\sim$30%. However, at increasing pump levels the upconversion process, as discussed earlier, becomes increasingly detrimental owing to its square dependence on the population of the upper laser level. The consequence is that it is nearly impossible to reach the exponential gain region using Cr:LiSAF. As shown in this

work and in previous experiments [10], [11] the amplification of Cr:LiSAF amplifiers is more or less linearly dependent on the pump energy, which makes it difficult to achieve single-pass amplifications of more than ~5.

C. Optical Damage and Self-Focusing

For the sake of completeness we would like to briefly mention the optical damage properties of Cr:LiSAF and Cr:LiCAF. Optical damage and self-focusing limits the output performance of laser/amplifier systems. First results to this issue have been recently published [6] giving bulk damage thresholds of 160 GW/cm^2 for 1.4% doped Cr:LiSAF and 400 GW/cm^2 for 2.5% doped Cr:LiCAF (at 1064 nm with a 47-ps-long pulse). Under the same conditions the optical damage of fused silica is 420 GW/cm^2. The nonlinear refractive indices of Cr:LiSAF and Cr:LiCAF at 1064 nm are ~5 and $\sim 4 \cdot 10^{-17}$ cm^2/W, respectively, which are significantly lower than that of fused silica of $3.2 \cdot 10^{-16}$ cm^2/W. The lower nonlinear refractive index of Cr:LiSAF and Cr:LiCAF allows higher energy extraction (per unit volume) from these materials than with Nd:glass amplifiers, avoiding small-scale self-focusing and its detrimental influence to the beam quality.

VI. Summary

We have reported small-signal gain measurements of Cr:LiSAF and Cr:LiCAF. The gain for both materials is moderate and is affected by ESA. We have made estimates of the ESA cross section of $1.6 \cdot 10^{-20}$ cm^2 for Cr:LiSAF at 850 nm and $3.2 \cdot 10^{-21}$ cm^2 for Cr:LiCAF at 785 nm. In the case of Cr:LiSAF, upconversion limits the pump efficiency at higher pump levels, making it difficult to achieve the regime of exponential gain with this material. Cr:LiSAF and Cr:LiCAF have a relatively efficient energy storage. Values of 1.6 and 3.6%, respectively, of stored energy in the upper laser level compared to the electrical input energy have been measured. Somewhat higher values can even be expected using laser heads specially designed to efficiently pump these materials.

Because of its broader spectral emission and its higher effective gain cross section, Cr:LiSAF is clearly the better choice for ultrashort high-energy pulse amplification. Single-pass amplifications of > 3 have been obtained using flashlamp-pumped Cr:LiSAF rod amplifiers [10], [11].As a rule, relatively large pump densities are required to overcome the drawback of ESA, and to reduce the effect of upconversion the use of long rods must be preferred. The gain of Cr:LiCAF is significantly lower than that of Cr:LiSAF, and it will be difficult to build optical amplifiers using this material. However because of its more efficient energy storage, its better mechanical and thermal properties, and higher gain saturation, Cr:LiCAF is the material of choice for efficient energy extraction using Q-switched laser systems without amplifiers.

Acknowledgment

The authors acknowledge the help of Lightning Optical Corporation and Schwartz Electro-Optics, useful discussions with Drs. S. A. Payne, M. Bass, V. Yanovsky, and X. Zhang, and the technical assistance of E. Miesak, C. Bogusch, T. DeLia, P. Reese, and J. Darnell.

References

[1] S. A. Payne, L. L. Chase, L. K. Smith, W. L. Kway, and H. W. Newkirk, "Laser performance of Cr:LiSAF," *J. Appl. Phys.*, vol. 66, pp. 1051–1054, 1989.

[2] S. A. Payne, L. L. Chase, H. W. Newkirk, L. K. Smith, and W. F. Krupke, "Cr:LiCAF: A promising new solid-state laser material," *IEEE J. Quantum Electron.*, vol. 24, pp. 2243–2252, 1988.

[3] P. F. Moulton, "Spectroscopic and laser characteristics of Ti:Al $_2O_3$," *J. Opt. Soc. Am. B*, vol. 3, pp. 125–133, 1986.

[4] J. C. Walling, D. F. Heller, H. Samelson, D. J. Harter, J. A. Pete, and R. C. Morris, "Tunable alexandrite lasers: development and performance," *IEEE J. Quantum Electron.*, vol. 21, pp. 1568–1581, 1985.

[5] B. W. Woods, S. A. Payne, J. E. Marion, R. S. Hughes, and Laura E. Davies, "Thermo-mechanical and thermo-optical properties of the Cr:LiCAF laser material," *J. Opt. Soc.*, vol. B8, pp. 970–977, 1991.

[6] M. C. Richardson, M. J. Soileau, E. Van Stryland, P. Beaud, Y.-F. Chen, R. DeSalvo, S. Garnov, D. J. Hagan, S. Klimentov, M. Shiek-Bahae, A. A. Said, and B. Chai, "Self-focusing and optical damage in Cr:LiSAF and Cr:LiCAF," *SPIE*, vol. 1848, to be published.

[7] L. DeLoach, S. A. Payne, L. K. Smith, J. B. Tassano, W. L. Kway, and W. F. Krupke, "Properties of the Cr:LiSAF laser crystal," *Proc. Ann. Mtg. Opt. Soc. Am.*, p. 32, 1992.

[8] M. Stalder, B. H. T. Chai, and M. Bass, "The flashlamp-pumped Cr:LiSrAlF$_6$ laser," *Appl. Phys. Lett.*, vol. 58, pp. 216–218, 1991.

[9] P. Beaud, E. Miesak, Y.-F. Chen, B. H. T. Chai, and M. C. Richardson, "A flashlamp pumped Cr:LiSAF regenerative amplifier," *OSA Proceedings on Advanced Solid State Lasers*, Lloyd L. Chase and Albert A. Pinto, eds., vol. 13, pp. 109–112, Washington, DC: Optical Society of America, 1992.

[10] M. D. Perry, D. Strickland, T. Ditmire, and F. G. Patterson, "Cr:LiSrAlF$_6$ regenerative amplifier," *Opt. Lett.*, vol. 17, pp. 604–606, 1992.

[11] W. E. White, J. R. Hunter, L. Van Woerkom, T. Ditmire, and M. D. Perry, "120-fs terawatt $TiAl_2O_3$/Cr:LiSrAlF$_6$ laser system," *Opt. Lett.*, vol. 17, pp. 1067–1069, 1992.

[12] P. Beaud, E. Miesak, Y.-F. Chen, B. H. T. Chai, and M. C. Richardson, "110 fs Fourier-transform limited Gaussian pulses from a Cr:LiSAF regenerative amplifier," *Optics Commun.*, vol. 95, pp. 46–50, 1993.

[13] T. Ditmire and M. D. Perry, "Terawatt Cr:LiSrAlF$_6$ laser," *Opt. Lett.*, vol. 18, p. 426, 1993.

[14] P. Beaud, M. Richardson, E. J. Miesak, and B. H. T. Chai, "8-TW, 90-fs, Cr:LiSAF laser," *Optics Letters*, to be published.

[15] R. Scheps, J. F. Myers, H. Serreze, A. Rosenberg, R. C. Morris, and M. Long, "Diode pumped Cr:LiSrAlF$_6$ lasers," *Opt. Lett.*, vol. 16, pp. 820–822, 1991.

[16] Q. Zhang, G. J. Dixon, B. H. T. Chai, and P. N. Kean, "Electronically tuned diode-laser-pumped Cr:LiSrAlF$_6$ laser," *Opt. Lett.*, vol. 17, pp. 43–45, 1992.

[17] R. Scheps, "Cr-doped solid state lasers pumped by visible diodes," *Optical Materials*, vol. 1, pp. 1–9, 1992.

[18] S. A. Payne, W. F. Krupke, L. K. Smith, W. K. Kway, L. D. DeLoach, and J. B. Tassano, "752nm Wing-Pumped Cr:LiSAF Laser," *IEEE Quantum Electron.*, vol. 28, pp. 1188–1196, 1992.

[19] S. A. Payne, L. L. Chase, and G. D. Wilke, "Optical spectroscopy of the new laser materials, Cr:LiSAF and Cr:LiCAF," *J. Luminescence*, vol. 44, pp. 167–176, 1989.

[20] K. I. Schaffers and D. A. Keszler, "Structure of LiSrAlF$_6$," *Acta Cryst.*, vol. C47, pp. 18–20, 1991.

[21] W. Viebahn, "Untersuchungen an quaternären Fluoriden LiMe"Me""F$_6$. Die Struktur von LiCaAlF$_6$," *Z. anorg. allg. Chem.*, vol. 896, pp. 335–339, 1971.

[22] Y.-F. Chen, P. Beaud, B. H. T. Chai, and M. C. Richardson, "Small signal gain measurements in Cr-doped LiSAF and LiCAF, *OSA Proceedings on Advanced Solid State Lasers*, L. L. Chase and A. A. Pinto, Eds., vol. 13, pp. 10–13, Washington, DC: Optical Society of America, 1992.

[23] W. R. Rapoport, "Excited-state absorption and upconversion in Cr:LiSAF," *OSA Proceedings on Advanced Solid State Lasers*, Lloyd L. Chase and Albert A. Pinto, eds., vol. 13, pp. 21–27, Washington, DC: Optical Society of America, 1991.

[24] P. Beaud, Y.-F. Chen, B. H. T. Chai, and M. C. Richardson, "Gain Properties of Cr:LiSAF," *Opt. Lett.*, vol. 17, pp. 1064–1066, 1992.

[25] M. A. Noginov, V. G. Ostroumov, I. A. Shcherbakov, V. A. Smirnov, and D. A. Zubenko, "Interaction of excited Cr^{3+} ions in laser crystals,"

OSA Proceedings on Advanced Solid State Lasers, H. P. Jensen and G. Dube, eds, vol. 10, pp. 21–24, Washington, DC: Optical Society of America, 1991.

[26] J. J. Kim, C.-M. Kim, J. Scheid, and B. H. T. Chai, "Cr^{3+}:$LiCaAlF_6$ laser pumped by a pulsed dye laser," *OSA Proceedings on Advanced Solid State Lasers,* Lloyd L. Chase and Albert A. Pinto, eds, vol. 13, pp. 5–9, Washington, DC: Optical Society of America, 1992.

[27] H. W. H. Lee, S. A. Payne, and L. L. Chase, "Excited-state absorption of Cr^{3+} in $LiCaAlF_6$: Effects of asymmetric distortions and intensity selection rules," *Phys. Rev. B,* vol. 39, pp. 8907–8914, 1989.

[28] S. A. Payne, Lawrence Livermore National Laboratory, PO Box 5508, Livermore, California 94550 (personal communication, 1992).

P. Beaud, photograph and biography not available at the time of publication.

M. C. Richardson, photograph and biography not available at the time of publication.

Y.-F. Chen, photograph and biography not available at the time of publication.

B. H. T. Chai, photograph and biography not available at the time of publication.